Catal Lett (2012) 142:71–80
DOI 10.1007/s10562-011-0738-4

Solvothermal Synthesis and Catalytic Properties of Nanocrystalline $ZnFe_{2-x}Al_xO_4$ (x = 0, 1, 2) Spinels in Aniline Methylation

Wiktoria Walerczyk · Mirosław Zawadzki · Hanna Grabowska

Received: 13 July 2011 / Accepted: 5 November 2011 / Published online: 19 November 2011

Abstract $ZnFe_{2-x}Al_xO_4$ (x = 0, 1, 2) spinels were obtained by microwave-assisted solvothermal method using 1,4-butanediol as reaction medium. The results of XRD and HRTEM studies have indicated higher nanocrystallinity of aluminium containing spinels, and N_2 adsorption–desorption measurements have revealed their enhanced textural properties, in particular much higher specific surface areas. NH_3-TPD method and cyclohexanol test have shown the variation of surface acid–base properties with the changes in the spinel composition. All studied spinels were active in aniline methylation and proved to be selective for N-methylation leading to *N*-methylaniline and *N*,*N*-dimethylaniline. The main advantage of aluminium containing spinels is that N-alkylation with methanol is possible at significantly lower temperature (200–260 °C) when pure zinc ferrite is almost inactive.

Keywords Spinels · Glycothermal method · Catalytic aniline N-methylation

1 Introduction

Alkylanilines such as *N*-alkyl and *N*,*N*-dialkyl derivatives of aromatic amines are important industrial chemicals and useful raw materials for organic synthesis as well as essential intermediates in the manufacture of many pharmaceuticals, fine chemicals, agrochemicals (insecticides, herbicides), explosives and dyes. Recently, some attention had been also paid to their application as octane number booster [1]. *N*-methylaniline (NMA) exhibits good antioxidant and antidetonant properties and is used as an intermediate in the synthesis of high energy materials and drugs [2, 3]. *N*,*N*-dimethylaniline (NNDMA) is a key precursor to commercially important triarylmethane dyes such as Malachite green and Crystal violet, serves as a promoter in the curing of polyester and vinyl ester resins. NNDMA is also used as a precursor to other organic compounds [4].

A number of methods are available for preparation of methylated derivatives of aniline (aminobenzene), the simplest of the primary aromatic amines. Generally, NMA and NNDMA can be synthesized either by a catalytic batch process in the liquid phase or by a flow process in the vapour phase in the presence of various catalysts. The first one is traditional route based on the application of corrosive acids or conventional Friedel-Crafts systems [5, 6], zeolites [7, 8], onium salts [9] as catalysts and alkyl halides or dimethyl sulphate as alkylating agents [10]. The second one is environmentally more benign process using solid catalysts such as metal oxides, aluminium and magnesium phosphates, clays, zeolites and others [11–22]. During catalytic aniline methylation, methanol as well as dimethyl carbonate (DMC) are used as alkylating agent [8, 23].

Because methylation reaction is a complex one with many side reactions, in both cases the formation of the target products is often accompanied by the formation of by-products including *C*-methylated anilines (toluidines), *N*-methylated toluidines or polymers [24] what may lead to catalyst deactivation. However, vapour phase process seems to be more attractive since reaction control for obtaining selectively *N*- or *C*-methylated anilines with high yields is less difficult and depends mainly on the reaction temperature and nature of the used catalyst. The current commercial production of *N*-methylated aniline uses, as the

W. Walerczyk (✉) · M. Zawadzki · H. Grabowska
Institute of Low Temperature and Structure Research, Polish Academy of Sciences, Okólna 2, 50-422 Wrocław, Poland
e-mail: wiktoria.walerczyk@int.pan.wroc.pl

main process, the vapour phase catalytic alkylation with methanol. Unfortunately, there is not much information on the use of industrial catalysts. There are some quotes published in the work of Stytsenko et al. [25]. According to data published in Stytsenko et al. [25], the industrial synthesis of *N*-methylated aniline in the vapour phase is performed over catalysts containing active copper and manganese oxides on alumina or in the presence of supported niobic acid.

Several studies on vapour phase methylation of aniline on mixed metal oxides with spinel structure as catalysts have been reported [26–31]. Mixed oxides with spinel structure are very interesting materials for alkylation reactions because their catalytic effectiveness for this type of reactions can be easy modified by introducing of the third metal into the spinel structure leading to the change of their acid–base nature. It was already demonstrated that adequate selection of substituting ion and appropriate chemical composition can change or modify the ions distribution in the spinel and therefore its catalytic properties for many reactions [32–36]. Although there are reports on using Zn, Co, Cr, Cu and Mn based ferrospinels but no information seems to be available on the behaviour of $Zn(FeAl)O_4$ system in this reaction. So far, one can find only a few papers that describe the aforesaid system and show its catalytic activity [32, 33, 37]. Reddy et al. [37] have carried out the methylation of phenol over $ZnFe_{2-x}Al_xO_4$ ferrospinel catalytic system and demonstrated its effectiveness in synthesis of 2,6-xylenol received with high yield and selectivity which was dependent on content of the Al ions.

Moreover, another important attribute of spinel materials is that this kind of structure provides high stability and catalytic life-time. Solid state reactions cannot usually provide materials with enough textural properties to induce appropriate catalytic properties. Recently, the solvothermal methods have become popular due to their mild conditions and facile processes which allow to obtain products characterized by very interesting textural properties (including sufficiently higher surface area, e.g. 290 m^2/g for $ZnAl_2O_4$ after heat treatment at 100 °C [38]), superior thermal stabilities and well-controlled chemical composition, which may provide higher potential for catalytic applications as compared to corresponding materials prepared by more traditional methods.

In our previous work [39], microwave-assisted glycothermal method was successfully used to synthesise nanosized spinel type mixed oxide containing Zn, Al and/or Co ions and all studied spinels were found to be active in phenol methylation but Co-substituted zinc aluminate ($Zn_{0.5}Co_{0.5}Al_2O_4$) was the most efficient in the selective formation of *ortho*-methylated products. It was therefore decided to prepare under the same conditions another spinel-type system containing Zn, Fe and/or Al ions with the aim to undertake investigation of vapour phase alkylation of aniline using methanol as the alkylation agent. Besides, such prepared catalysts have been characterized by XRD, TEM, nitrogen adsorption–desorption measurements, NH_3-TPD and cyclohexanol tests (CHOL tests) to find the relationship between their physico-chemical properties (structure, texture, acid–base nature) and the catalytic behaviour.

2 Experimental

2.1 Catalysts Preparation

In the present study, various spinel compositions viz. $ZnAl_2O_4$, $ZnFeAlO_4$ and $ZnFe_2O_4$ were prepared using microwave assisted glycothermal method. Initially, calculated stoichiometric amounts of zinc acetate and/or ferric citrate were added to distilled water and mixed with magnetic stirrer for ca. 5 min until they were completely dissolved. Next, a proper amount of aluminium isopropoxide was suspended in 99% 1,4-butanediol and mixed together in the desired weight ratios with prepared earlier water solution of Zn and/or Fe salts. So prepared solutions of metal precursors were put into a Teflon vessel and placed in an autoclave with microwave heating. Reaction was provided for 60 min (including the time needed to heat up the sample) at 200 °C under autogenic pressure of ~30 atm. Each resulting material was washed several times with acetone (to remove organic residues) and centrifuged. After that, the obtained gel was extruded to form wires with diameter ~3 mm, air-dried overnight at room temperature (RT) and after heating from RT to 550 °C (with dynamic heating rate amounted ~10 °C/min) calcined in static conditions at 550 °C for 3 h. Next, so prepared samples were crushed and sieved (16–30 mesh size). The samples were labelled as ZFO, ZFAO and ZAO for $ZnFe_2O_4$, $ZnFeAlO_4$ and $ZnAl_2O_4$, respectively. The obtained catalysts were characterized by physico-chemical methods and their catalytic activity was tested in the reaction of aniline methylation.

2.2 Characterization Techniques

Crystalline phase identification and average grain size calculations were done using Powder X-Ray Diffraction. XRD measurements were performed employing X'Pert Pro Panalytical diffractometer using Ni-filtered radiation (CuK_α, $\lambda = 1.5406$ Å) in the 2θ range from 10 to 80°. X'Pert HighScore Plus software equipped with PDF2 data base was used for phase composition identification, cell-parameter calculation for the spinel phase and average crystallite size calculation using Scherrer's equation.

Samples morphology and microstructure of the synthesised products were analyzed by High Resolution Transmission Electron Microscopy (HRTEM) and Selected Area Electron Diffraction (SAED). HRTEM images and SAED patterns were recorded on Philips CM20 SuperTwin microscope operated at 200 kV with 0.25 nm resolution, and equipped with CCD camera. Studied samples were ground in a mortar, suspended in methanol, and then dispersed ultrasonically. One drop of the suspension was placed on a carbon coated copper grind and allowing the solvent to evaporate.

Textural properties including porosity and specific surface area were measured by nitrogen adsorption–desorption method at liquid nitrogen temperature. The measurements were carried out using an Autosorb-1 Quantachrome Instruments automated system after sample degassing at 200 °C for 2 h. The specific surface area S_{BET} was determined from the adsorption data using Brunauer–Emmet–Teller (BET) method while pore size distribution was calculated using the Barret–Joyner–Halenda (BJH) method. The mean pore size (D_{pore}) corresponds to maximum of pore size distribution curve.

The total surface concentration of acid sites and acidity strength distribution were determined using a temperature programmed desorption of ammonia (NH_3-TPD). The sample (2 g) was heated from RT up to 550 °C in argon flow for 1 h and next cooled to 180 °C. Adsorption of pure ammonia was performed for 0.5 h followed by a purge with argon at 180 °C for 1 h to remove physically adsorbed NH_3. Finally, NH_3-TPD measurements were started in argon with a heating rate of 10 deg/min. Amounts of desorbed ammonia was measured using gas chromatograph with a TCD detector.

Acid-basic properties were determined by analysis of results of cyclohexanol (CHOL) decomposition. CHOL dehydrogenation to cyclohexanone (CHON) takes place on acid as well as basic centres, but cyclohexene (CHEN) is obtained only on acid centres. Therefore, decomposition of CHOL to CHEN is the measure of the surface's acid strength while the ratio of CHON/CHEN selectivities gives information about basic nature of materials [40]. It is assumed that the dehydration and dehydrogenation processes represent a set of parallel reactions. The measurements of catalytic activity in CHOL decomposition were carried out in a continuous-flow fixed bed quartz reactor with electric heating. The catalyst (0.1 g) mixed with SiC (to 1 cm^3 volume) was held on quartz wool. During reaction total gas flow was set on 10 dm^3/h (dry N_2 99.999% saturated with 2.6 mmol/h of CHOL) and reaction temperature was set on 400 °C. Distribution of the reaction products was analysed using gas chromatograph equipped with FID detector. The obtained results were used to calculate the total conversion of CHOL and selectivities to CHEN and CHON.

2.3 Catalytic Methylation of Aniline

The experiments of aniline alkylation with methanol were carried out continuously in a standard quartz down flow fixed-bed vertical reactor (6 mm i.d.) surrounded by an electric heater in the temperature range 200–360 °C. The temperature was continuously controlled with a thermocouple placed in the middle of the catalyst bed, and the unit was operated at atmospheric pressure. The fixed bed containing of 3 cm^3 of catalyst was placed on quartz wool at the centre of the reactor. The substrate (an aniline solution in methanol with an addition of water with molar ratio 1:5:1, respectively) was fed in a continuous manner to the reactor from the top by a dosing pump at a flow ratio of 1.5 cm^3 liquid/h (Liquid Hourly Space Velocity—LHSV = 0.5 h^{-1}) and was vaporised before it was passed through the catalyst bed, without presence of carrier gas. Water was added to the aromatic-alcohol mixture of reactants to prolong the activity of the catalysts during the reaction of methylation [41–44]. The reactions were performed as a function of temperature, mole ratios of the reaction mixture, feed rates (LHSV—varied from 0.7 to 1.8 h^{-1}) and time-on-stream. Catalysts were firstly activated during 2 h in the flow of the reactants mixture at temperature up to 200 °C. The experiments were carried out for 1–2 h under steady conditions at chosen temperatures, and collected products were analysed on a HP 6890 GC equipped with a flame ionization detector and with a 5% phenyl methyl siloxane capillary column (30 m × 0.32 mm × 0.25 µm) and helium as a carrier gas. NMA and NNDMA were the main compounds detected in the reaction products. The conversion of aniline was defined as a fraction of reacted aniline, whereas the selectivity was obtained on the basis of the percentage of the given alkyl anilines in the liquid reaction products. A blank run without any catalyst indicated negligible thermal conversion.

3 Results and Discussion

3.1 Catalysts Characterization

The XRD patterns of studied samples are given in Fig. 1 and show that all diffraction peaks match well to the characteristic reflections of face centred cubic spinel type structure. The XRD measurements indicate absence of segregated oxide phases (ZnO, Al_2O_3 or Fe_2O_3) and confirm the phase purity of the samples prepared under solvothermal conditions.

It can be seen from Fig. 1 that the diffraction peaks are broad and their broadening increases with aluminum content increasing, as a result, the mean crystallite size should decrease with increasing of aluminium content.

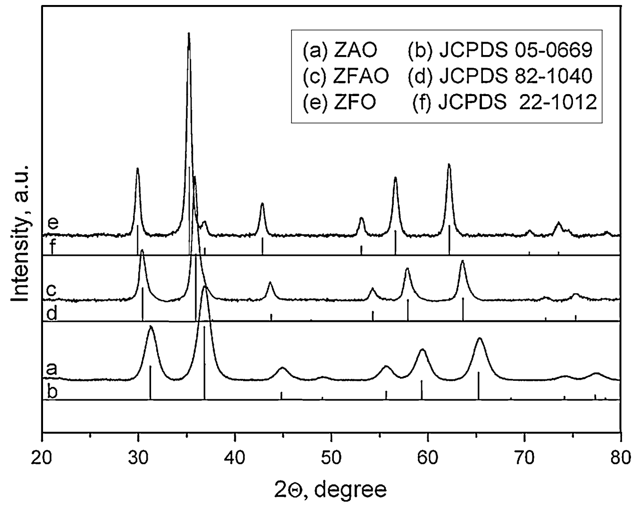

Fig. 1 XRD patterns of spinels (*a*) ZAO, (*c*) ZFAO, (*e*) ZFO with corresponding data for (*b*) $ZnAl_2O_4$, (*d*) $ZnFeAlO_4$ and (*f*) $ZnFe_2O_4$

ZAO sample (Fig. 1a) shows major diffraction peaks at $2\theta = 31.3°$, 36.9°, 44.9°, 55.7°, 59.4°, 65.4°, 74.3° and 77.4° which are characteristic for (220), (311), (400), (422), (511), (440), (620) and (533) lattice plane of zinc aluminate structure (JCPDS 05-0669) while in the pattern of ZFO sample (Fig. 1c) well visible are peaks at $2\theta = 29.9°$, 35.2°, 36.8°, 42.8°, 53.0°, 56.6°, 62.2°, 70.5° and 73.5° originating from (220), (311), (222), (400), (422), (511), (440), (620) and (533) lattice plane of zinc ferrite (ZFO) (JCPDS 22-1012). For ZFAO sample, however, one can observe that diffraction peaks are shifted towards higher 2θ angles in comparison to corresponding ones of ZFO sample suggesting the incorporation of aluminium ions into the structure of ZFO and is correlated with bigger ionic radius of Fe^{3+} (0.64 Å) than Al^{3+} (0.50 Å). All diffraction peaks for this sample (Fig. 1b) match well to the reflections of $Zn(FeAl)O_4$ system reported in the JCPDS File No. 82-1040. Diffraction pattern of ZAO sample exhibits very broad peaks indicating on small crystallite sizes while for ZFAO and ZFO samples they are sharper suggesting higher crystallinity. The average crystallite sizes calculated from Scherrer's equation using the FWHM of the reflection plane (311) amount to 6, 10 and 15 nm, respectively, for ZAO, ZFAO and ZFO sample (Table 1). The data included in Table 1 show also decrease of lattice parameters (unit-cell parameter and volume) for ZFAO and ZAO samples due to the incorporation of Al^{3+} ions with smaller ionic radius into the spinel structure.

The morphology and particle size distribution of studied samples were characterized by HRTEM technique while SAED patterns were used to phase identification. Typical HRTEM micrographs with corresponding SAED patterns are collected in Fig. 2. Analysis of micrographs of ZAO sample (Fig. 2a) indicates on nanosize character of this sample, with crystallite diameter in the range of 3–8 nm. Shape of crystallites is rather uniform and quasi-spherical and one should notice that they form aggregates consisting of many particles. Well visible are diffraction fringes with d-spacing around 0.29 nm corresponding to (220) lattice plane of zinc aluminate structure. Analysis of SAED patterns confirms spinel structure of ZAO, diffraction rings shown as inset to Fig. 2a could be indexed to (220), (311), (400), (422) and (511) lattice planes of $ZnAl_2O_4$, what is consistent with the HRTEM observation and XRD data.

Table 1 Structural and textural properties of studied spinels

Catalyst	ZAO	ZFAO	ZFO
d_{XRD} (nm)	6	10	15
Lattice parameters			
a (Å)	8.080 (1)	8.305 (6)	8.443 (9)
α (°)	90	90	90
V (Å^3)	527.61	572.81	601.95
S_{BET} (m^2/g)	152	116	32
V_{total} (cm^3/g)	0.34	0.42	0.13
D_{pores} (nm)	6.3	11.7	12.6

Images of ZFO sample exhibit higher crystallinity what could be noticed in Fig. 2c as well as broader range of distribution of crystallite sizes. It is well seen that some part of crystallites is visible bigger than the rest. Average particles size for this sample calculated from HRTEM images amounted to 18 nm. SAED patterns confirm the presence of $ZnFe_2O_4$ with spinel structure: the major rings are characteristic for (111), (220), (311), (400), (422), (511) and (440) lattice plane of ZFO.

HRTEM image of ZFAO sample is presented in Fig. 2b. It should be noticed that crystallites are bigger and less uniform in shape than in ZAO sample and particles size is in the broader range, namely 5–15 nm. Average crystallite size, 9 nm, is in a good agreement with XRD data. Diffraction rings in SAED patterns exhibit d-spacing 0.29, 0.25, 0.20, 0.17, 0.16 and 0.13 nm characteristic for zinc aluminate spinel structure in which about half of Al ions were substituted by Fe ions.

Texture characteristic of studied samples was determined using N_2 physisorption method. N_2 adsorption and desorption isotherms and corresponding pore size distribution of ZAO, ZFAO and ZFO are given in Fig. 3. The isotherms are characteristic for type IV in accordance with IUPAC classification what indicate the mesoporous nature of studied samples. Moreover, it is well seen that isotherms have hysteresis shape of type H1 (Fig. 3a, c) or H3 (Fig. 3b) according to IUPAC classification. The H1 type is observed in the case of pores with uniform size and shape

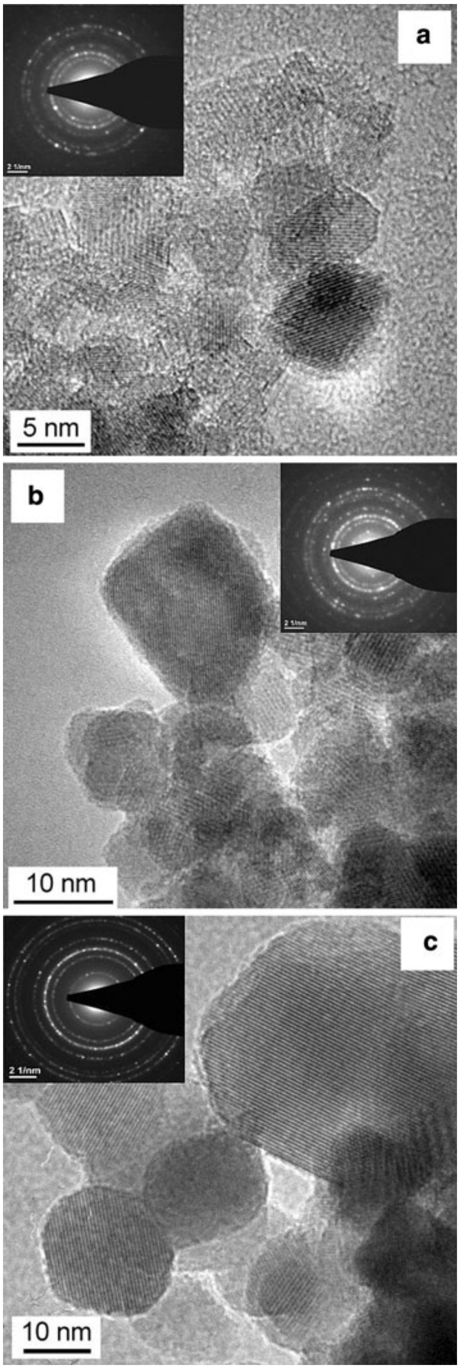

Fig. 2 HRTEM images of **a** ZAO, **b** ZFAO and **c** ZFO spinels with SAED patterns shown as *insets*

formed by aggregates, agglomerates or particles crossed by nearly cylindrical channels. The H3 hysteresis type is characteristic for slit shaped pores with non-uniform size and/or shape formed from aggregated or agglomerated particles. The values of the specific surface area calculated using the BET method (S_{BET}), pore size diameter calculated according to BJH method (D_{pores}) and total pore volume (V_{total}) are summarized in Table 1.

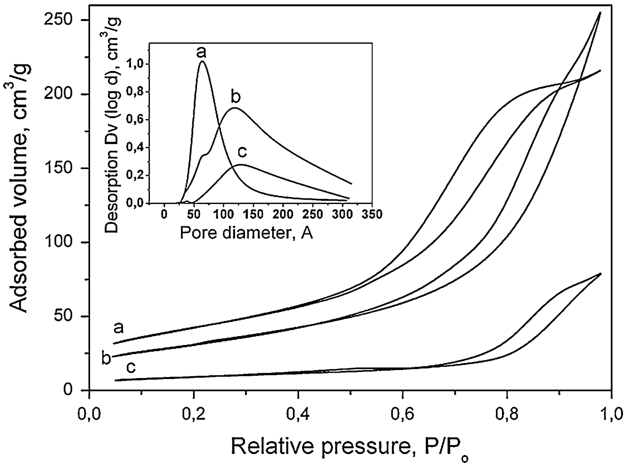

Fig. 3 N_2 adsorption–desorption isotherms of (*a*) ZAO, (*b*) ZFAO and (*c*) ZFO spinels with corresponding pore size distributions (as an *inset*)

It can be noticed that S_{BET} and V_{total} were significantly lower for ZFO than for aluminium containing spinels. The observed decrease in S_{BET} can be attributed to the increase in the particles size. The same behaviour after the Al^{3+} ions incorporation into the structure of ZFO, i.e. increase of S_{BET} with increasing of aluminium substitution degree, was already reported in the literature [37]. The pore size distribution curves presented as a inset in Fig. 3 show that ZAO exhibits narrow pore size distribution whereas ZFAO and ZFO show visible broader distribution of pore diameter. Moreover, the maximum share of pore size for ZAO is much lower than for iron containing catalysts.

It is well known that nature, number and distribution of acid sites is a key factor in the reaction of hydroxyarene alkylation by alcohols, also in aniline methylation. Thus, acid properties of tested samples were estimated by NH_3-TPD method considering amount of NH_3 desorbed at given temperature range and total amount of desorbed ammonia as acid strength and total number of acid sites, respectively. Ammonia desorbs from three type of centres: weak, medium and strong ones at different range of temperatures: below 200 °C, 200–400 °C and above 400 °C, respectively. Amount of acid sites calculated from TPD profile is given as mmol of NH_3 desorbed from 1 g of catalyst.

Figure 4 shows the distribution of acid centres for studied catalysts while the total amounts of desorbed ammonia are summarized in Table 2. The total acidity of studied samples increases in the following order: ZFO < ZFAO < ZAO, i.e. with increasing of Al content. All samples show a small amount of weak centres. ZAO and ZFAO samples exhibit a little higher content of this kind of acid sites than ZFO but in the reference to the total acidity—the weak ones comprise <2% in all cases. The highest amount (per gram) of acid centres with medium strength shows ZAO sample. The medium ones comprise

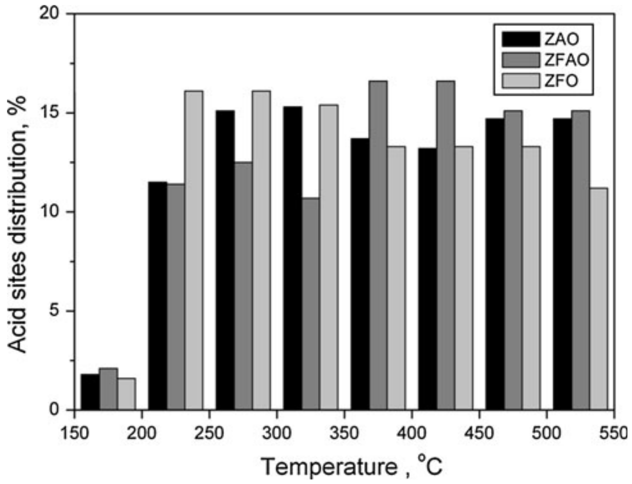

Fig. 4 Acid sites distribution (NH_3-TPD method)

Table 2 Acidity properties measured by NH_3-TPD method

Catalyst	NH_3 desorption (mmol NH_3/g)			
	Weak	Medium	Strong	Total acidity
ZAO	0.013	0.406	0.311	0.73
ZFAO	0.013	0.328	0.300	0.64
ZFO	0.005	0.188	0.117	0.31

55.6, 51.2 and 60.6% of total acidity of ZAO, ZFAO and ZFO, respectively. Zinc aluminate catalyst shows also the highest amount of strong acid sites per gram, but in this case difference between ZAO and ZFAO sample is significant smaller. The strong acid centres amount to 42.6, 46.9 and 37.7% of total acidity of ZAO, ZFAO and ZFO, respectively. It clearly demonstrated that there is less percentage contribution of strong acid sites on the surface of pure ZFO.

CHOL tests specify the acid-basic properties of the studied materials. The percentage conversion, product selectivity and ratio of CHON and CHEN selectivities during CHOL decomposition over the studied systems are collected in Table 3.

Tests of CHOL conversion demonstrate that ZAO catalyst is the most active in the midst of studied materials. Among the studied samples the dehydration activity varies in the order ZFO < ZFAO < ZAO, whereas the dehydrogenation activity follows the opposite order. The highest selectivity to CHON obtained over ZFO catalyst indicates on dominate basic character of this sample. The similar, but little bit lower result was observed for ZFAO material. The changes in basicity show an decreasing trend with progressive substitution of iron by aluminium. The highest conversion of CHOL and the highest selectivity to CHEN achieved in the presence of ZAO catalysts shows the strongest acidic properties of that sample. Differences in results obtained in CHOL conversion between all studied $ZnFe_{2-x}Al_xO_4$ (x = 0, 1, 2) samples are probably due to the changing spinel surface caused by the partial substitution of Fe by Al ions.

Table 3 Results of cyclohexanol decomposition

Sample	ZAO	ZFAO	ZFO
Conversion of CHOL[a] (%)	8.9	4.8	5.3
Selectivity to CHEN[b] (%)	20.7	13.0	10.4
Selectivity to CHON[c] (%)	79.3	87.0	89.6
$Sel._{CHON}/Sel._{CHEN}$	3.8	6.7	8.6

[a] Cyclohexanol

[b] Cyclohexene

[c] Cyclohexanone

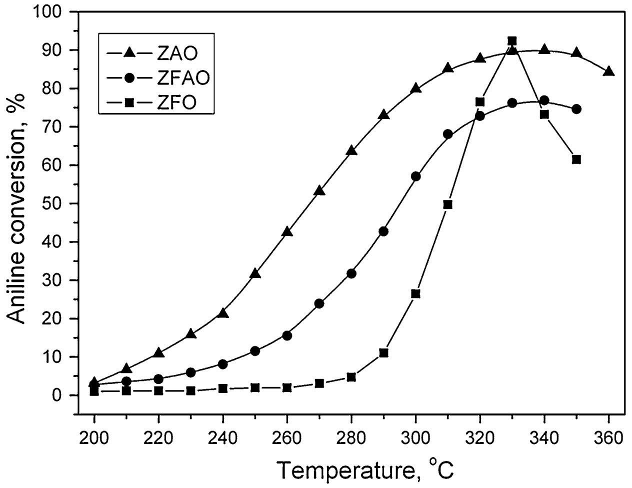

Fig. 5 Comparison of aniline conversion over glycothermally synthesised ZAO, ZFAO and ZFO spinels in N-methylation reaction

Based on the results of measurements of acidity, both by NH_3-TPD and CHOL tests, it can be concluded that the addition of Al ions into the spinel structure increases the total acidity as well as density of weak, medium and strong acid sites with simultaneous decrease of basic properties.

3.2 Catalytic Activity

The catalytic properties of ZAO, ZFAO and ZFO were examined in the reaction of aniline alkylation with methanol. Reaction was carried out in the vapour phase at atmospheric pressure in the temperature range of 200–360 °C. Temperature-dependent catalytic activity measurements—the aniline conversion and yields of main reaction products—obtained at 1:5:1 molar ratios of reagents (aniline: methanol:water, respectively) and at load (LHSV) = 0.5 h^{-1} are shown in Figs. 5 and 6, respectively. Additionally the influence of the reaction temperature upon the N-methylation selectivity was also demonstrated in Fig. 6.

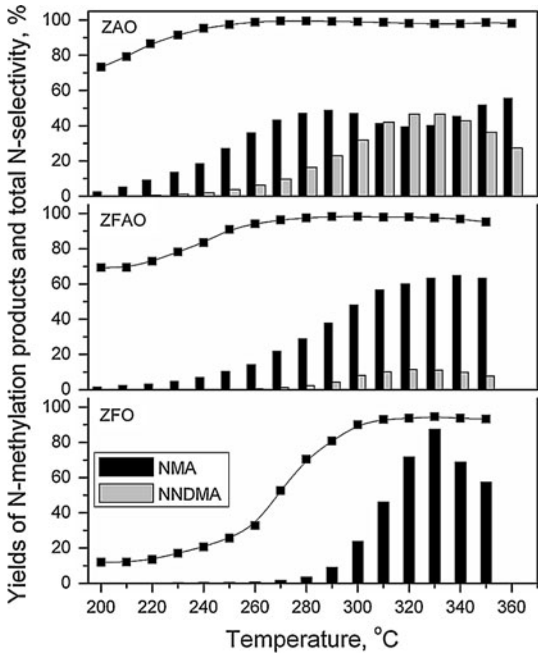

Fig. 6 Temperature dependence of yields of aniline methylation products and total N-selectivity for ZAO, ZFAO and ZFO catalysts

All studied catalysts are active for aniline methylation. The conversions reported here are on methanol free aniline basis. In the cases of all catalysts an increase in the reaction temperature increases the aniline conversion. It should be noted that an efficient activity was observed for Al containing spinels already at low temperatures (220–260 °C), while for pure ZFO only at significant higher temperatures (>290 °C). The maximum aniline conversion was achieved at 330–340 °C in the presence of all examined materials. For ZFO catalyst the obtained activity pattern is a volcano-type with temperature and this material exhibited the highest value of aniline conversion (up to 92.4% at 330 °C). Almost 90% of aniline conversion was stated on ZAO catalyst at 340 °C, whereas ~77% of aniline conversion was achieved over ZFAO at the same temperature. It should be noted that only moderate acidity is required for a good catalytic reactions between aniline and methanol, as was previously observed for other Fe/Al containing materials [45]. On all studied catalyst, after stopping the reaction, cooling down, and starting all over again, almost the same conversions level were attained at almost the same temperatures, as previously had been noted.

The liquid reaction products consist of unreacted aniline, *N*-methylated aniline derivatives (NMA, NNDMA) and small amount of toluidines. The last ones were not identified. The yields of main N-methylated reaction products and the curves of total N-methylation selectivities obtained in the presence of examined catalysts during methylation reaction in the function of temperature are shown in Fig. 6. NMA was formed as the major product over all catalysts samples. However, in the presence of ZFO only NMA was obtained with 87.4% of yield and the conversion was stated at the highest temperature. When ZAO and ZFAO were used the multistep sequential reactions of methanol with aniline gave NMA and NNDMA as main reaction products. These two products can be formed by the direct electrophilic substitution of methyl group on the nitrogen atom. In the presence of ZFAO and ZAO catalysts the yield of NMA reached 64.7 and 42.8%, respectively, while NNDMA was obtained with the yield of 11.4% on ZFAO and 46.6% on ZAO. The maximum yield of N-methylated products (at 330 °C) was almost the same for all catalysts indicating that not total surface acidity is responsible for the catalytic activity of studied spinels but the presence of acid sites with suitable strength and concentration. In the case of ZAO catalyst with the highest distribution of strong acid sites, NMA can also be formed by the *trans*-alkylation reaction of adsorbed NNDMA molecules and aniline [46]. Therefore, strong acid sites—not required for the N-alkylation of aniline—seems to be responsible for the transalkylation of aniline with NNDMA.

All studied catalysts are selective in the reaction of aniline N-methylation but ZAO and ZFAO are highly selective already at low temperature range. Moreover, it should be noted that the highest total selectivities to N-methylated products (up to 99% in the case of ZAO and 96–98% for ZFAO) were obtained when aluminium containing spinels were used as catalysts. ZFO catalyst exhibited N-selectivity up to 94.5% but only towards NMA. It is in accordance with expected trend that catalyst with lower acidity exhibit higher selectivity towards formation of mono-N-alkylated products [5].

Figure 7 illustrates the effect of time-on-stream (TOS test) on the aniline conversion and the product yields at 310 °C, atmospheric pressure, methanol to aniline molar ratio of 5 and feed rate 1.5 cm^3/h (LHSV = 0.5 h^{-1}). Only in the case of ZAO catalyst the aniline conversion and each of the yields of NMA and NNDMA increased slightly during the initial 2 h on stream and thereafter remain stable. Figure 7 for ZFAO shows that there was no change in aniline conversion and the yields of each N-methylated products also remained almost unchanged during a few hours. All studied catalysts displayed almost the same behaviour, so there is apparently no deactivation of the catalysts due to coke deposition at the reaction temperature of 310 °C. The calculated total selectivity of N-methylation in the TOS tests attained a high value of 95–96, 98 and 95–97% for ZAO, ZFAO and ZFO, respectively, during the whole period of studied time. It should be mentioned, however, that the catalysts stability is significantly improved by suppressing the side reactions of methanol gasification by adding water to the reaction mixture.

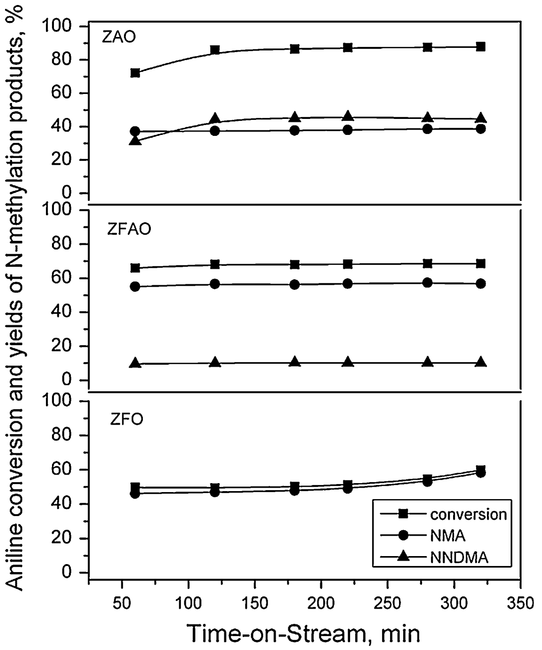

Fig. 7 Effect of time-on-stream on the conversion of aniline and yields of N-methylated products at 310 °C

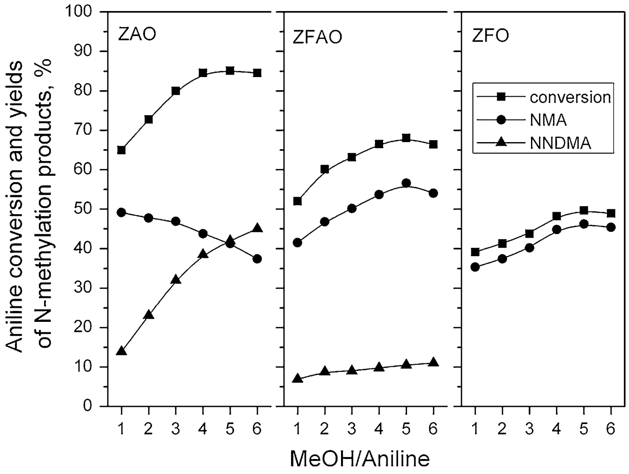

Fig. 8 Effect of methanol to aniline molar ratio on aniline conversion and yields of N-methylation products over ZAO, ZFAO and ZFO catalysts at 310 °C

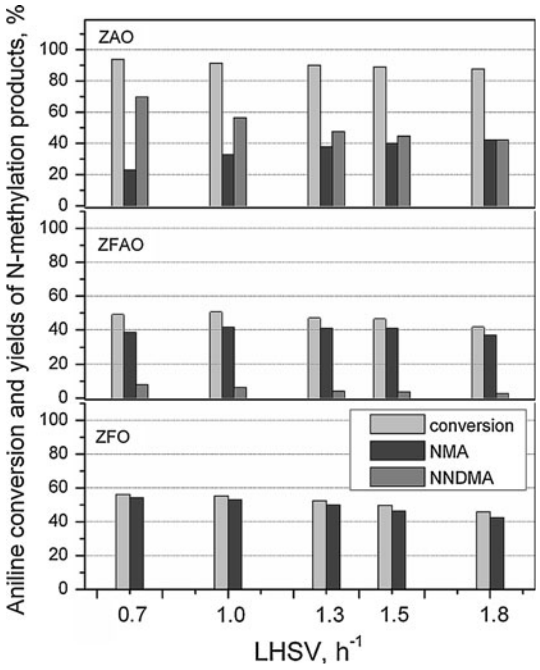

Fig. 9 Effect of feed rate on conversion and selectivity of aniline methylation over ZAO, ZFAO and ZFO catalysts at 310 °C

In order to understand the optimum feed mix ratio a series of experiments were performed at different molar ratios of methanol to aniline (MeOH/An) in the studied reaction of aniline methylation at 310 °C and at LHSV = 0.5 h^{-1}. Figure 8 shows the influence of methanol/aniline molar ratio on the aniline conversion and the product yield. In all cases NMA has been formed as a major product. For ZAO catalyst, as the MeOH/An ratio increases, the aniline conversion increases reaching maximum at MeOH/An = 5. At substrates ratio equal 1 the main reaction product is NMA. Further increase in the molar ratio decreased the yield of NMA with corresponding increase the yield of NNDMA. This suggests that at higher molar ratios, the consecutive methylation to NNDMA is preferred. The same trend was observed and reported by Ko et al. [12]. For ZFAO catalyst an increase in MeOH/An molar ratio causes gentle increasing aniline conversion as well as yields of NMA and NNDMA. The similar behaviour was observed when ZFO catalyst was used, but in this case no NNDMA production was observed. For all catalysts a maximum conversion of aniline has been found for MeOH/An = 5. In that case the aniline conversion reached 85.1, 68.1 anf 49.7% for ZAO, ZFAO and ZFO catalysts, respectively.

The influence of LHSV on conversion of aniline, and yields of NMA and NNDMA over studied spinels at 310 °C and a MeOH/An molar ratio 5 was also studied and results are shown in Fig. 9. Aniline conversion with respect to flow rate shows the same tendency in all cases, and with increase in LHSV it slightly decreases on ZAO, ZFAO and also on ZFO. At higher flow rate the catalysts possessing iron gave lower yields of N-methylated products. The more visible changes in the yields of NMA and NNDMA in the function of LHSV were observed for ZAO catalyst. In this case, the yield of NMA increases with LHSV and from 1.3 h^{-1} remains almost steady at higher feed rates. The opposite trend was observed for the obtained NNDMA. Low feed rate and thus high contact time favours secondary product (NNDMA) formation.

Alkylation is an electrophilic substitution reaction. Aniline is strong base and can interact even with the weak acid sites. Due to the adsorption of aniline on the surface of the catalyst, alkylation usually yields N-alkylated products. Free methanol (alkylating agent) is unreactive substrate and does not display any electrophilic reactivity. To transform it into reactive electrophile it must react with an acidic site of the catalyst. The catalyst plays a major role in discharge the active electrophile from the alcohol and therefore adsorption of alcohol is more significant. The electrophile—carbenium ion ($CH_3^{\delta+}$)—is formed from methanol with the help of the acid sites on the catalyst surface. Both reagents—aniline and methanol—are adsorbed on neighbouring sites and are in equilibrium with the catalyst surface. The electrophilic attack of the carbenium ion on the nitrogen atom of aniline results in favourable formation of NMA which can be subsequently converted into NNDMA. Due to presence of electron donating methyl group on nitrogen atom the adsorption of NMA is more probable over the catalyst surface than aniline. Since basic sites (in opposite to acidic ones) inhibited the strong adsorption of NMA to obtain NNDMA, thus the most basic catalyst (in our case ZFO) produced only NMA. Based on above general considerations commonly accepted for metal oxides catalysts in the reaction of aniline methylation, a reaction pathway is illustrated in Fig. 10. Therefore, acid–base properties of catalysts' surface play a crucial role in the reaction of aniline methylation and should be taken into account to explain their activity, products distribution and selectivity in studied reaction. It is assumed, according to Jacobs et al. [47], that surface layer in the spinel lattice is mainly octahedral, i.e. octahedral cations are expected to be exposed on the surface whereas the tetrahedral ones may be not easy of access, and acidity of spinels surface is mostly dependent on the nature of octahedral cations. Therefore, it is clear that adsorption and subsequent reaction of aniline with methanol should be sensitive to the substitution of cations into the octahedral sites of the spinel structure. Progressive substitution of Fe^{3+} ions by Al^{3+} ions creates an increase in acidity with the simultaneous decrease in basicity of the system [37]. However, it is known from the literature data that acidity and activity in the alkylation of aniline are not well-correlated and that the change in the basicity of the system rather than acidity may be this factor which control the overall performance of the catalysts [16, 48]. In our case, an increase in acidity is reflected in the aniline methylation activity mostly at low temperatures. At 220–270 °C range, only catalysts containing aluminum ions (ZAO and ZFAO) are highly active giving both N-mono and N,N-dialkylated products. Thus, this activity can be accounted due to the increase of total acidity and higher distribution of strong acid sites with concomitant removal of basic centers originally present on ZFO catalyst by aluminum substitution. Moreover, structural distortions resulting from the substitution of Fe^{3+} by Al^{3+} ions was extended to the surface modifying the textural properties giving considerable increase in specific surface area. ZAO, with the largest surface area seems then to posse optimum acid–base sites that are well suited for the proper adsorption and subsequent polarization of the N–H bond at low temperature. At higher temperatures, aniline conversion and total yield of N-methylated products were high for all studied catalysts, but selectivity towards NMA formation was much higher for the iron containing catalysts. At temperature of maximum activity (330–340 °C), only pure ZFO was able to give monomethylated product.

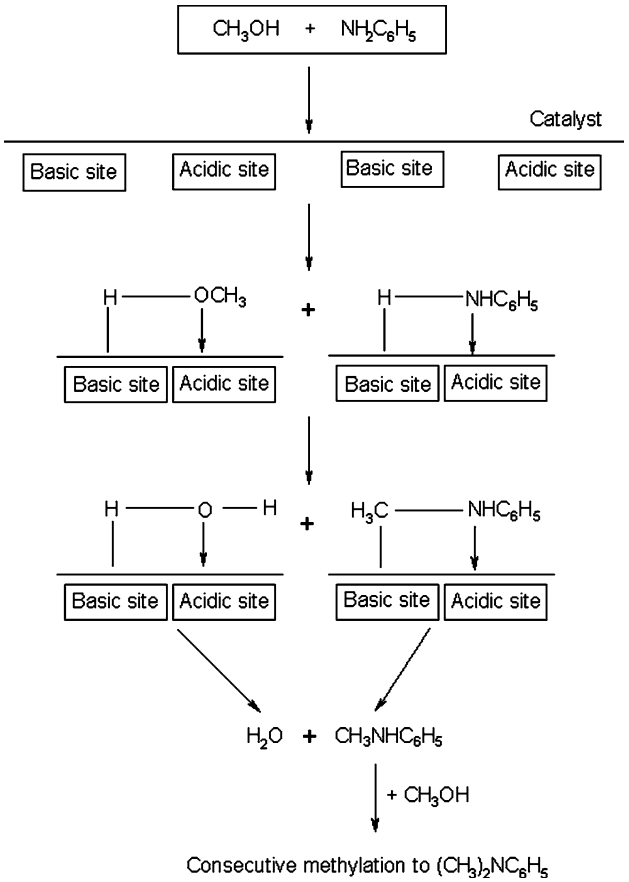

Fig. 10 Reaction pathway for aniline methylation

4 Conclusions

Substitution of Fe^{3+} by Al^{3+} ions in the $ZnFe_{2-x}Al_xO_4$ (x = 0, 1, 2) spinels under microwave-assisted glycothermal conditions leads to enhanced nanocrystallinity and textural properties of such system and changes its acid–base properties. All spinels are active in N-methylation of aniline with methanol as alkylating agent. $ZnAl_2O_4$ and

$ZnFeAlO_4$ afforded both mono- and di-substitution on the nitrogen of aniline leading to lower selectivity towards NMA. $ZnFe_2O_4$ produced NMA as only one N-methylated reaction product. The main advantage of aluminium containing spinels is that N-alkylation with methanol is possible at significantly lower temperature when pure ZFO is almost inactive. In the case of all studied catalysts N-methylation selectivity reached above 90%, except that the highest total selectivity of *N*-methyl aniline derivatives formation showed ZAO throughout the whole temperature range. From reaction temperature of 260 °C it reached more than 97%. All the studied systems were fairly stable under the experimental conditions.

Acknowledgments This work is supported by Polish Committee for Scientific Research (Grant No. N N507 500738). The authors are very grateful to Mrs. Ludwina Krajczyk for HRTEM studies and to Mrs. Sylwia Sieradzka for NH_3-TPD and CHOL tests.

References

1. Ma HZ, Zhu ZG, Wang B (2008) Energy Fuels 22:2157
2. Immel O, Waldman H, Braden R (1991) GE Patent 3,942,413
3. Jyothi TM, Raja T, Talawar MB, Sreekumar K, Sugunan S, Rao BS (2000) Synth Commun 30:3929
4. Gessner T, Mayer U (2002) In: Elvers B, Hawkins S, Schultz G (eds.) Ullmann's encyclopedia of industrial chemistry, Wiley-VCH
5. Narayanan S, Deshpande K (2000) Appl Catal A Gen 199:1
6. Bhattacharya AK, Nandi DK (1975) Ind Eng Chem Prod Res Dev 14:162
7. Selva M, Bomben A, Tundo P (1997) J Chem Soc Perkin Trans 1:1041
8. Esakkidurai T, Pitchumani K (2004) J Mol Catal A Chem 218:197
9. Shivarkar AB, Gupte SP, Chaudhari RV (2005) J Mol Catal A Chem 226:49
10. Shreve NR, Vriens GN, Vogel DA (1950) Ind Eng Chem 42:791
11. Parera JM, González A, Barral MA (1968) Ind Eng Chem Prod Res Dev 7:259
12. Ko AN, Yang CL, Zhu WD, Lin HE (1996) Appl Catal A Gen 134:53
13. Valot F, Fache F, Jacquot R, Spagnol M, Lemaire M (1999) Tetrahedron Lett 40:3689
14. Narayanan S, Prasad P (1995) J Mol Catal A Chem 96:57
15. Oku T, Arita Y, Tsuneki H, Ikariya T (2004) J Am Chem Soc 126:7368
16. Bautista FM, Campelo JM, Garcia A, Luna D, Marinas JM, Romero AA (1998) Appl Catal A Gen 166:39
17. Aramendía MA, Borau V, Jiménez C, Marinas JM, Romero FJ (1999) Appl Catal A Gen 183:73
18. Nehate M, Bokade VV (2009) Appl Clay Sci 44:255
19. Santhanalakshmi J, Raja T (1996) Appl Catal A Gen 147:69
20. Luque R, Campelo JM, Luna D, Marinas JM, Romero AA (2007) J Mol Catal A Chem 269:190
21. Ono Y (1997) CATTECH 3:31
22. Ivanova II, Pomakhina EB, Rebrov AI, Hunger M, Kolyagin YG, Weitkamp J (2004) J Catal 203:375
23. Nagaraju N, Kuriakose G (2003) New J Chem 27:765
24. Park YK, Park KY, Woo SI (1994) Catal Lett 26:169
25. Stytsenko VD, Huu TD, Vinokurov VA (2005) Kinet Catal 46:376
26. Sreekumar K, Jyothi TM, Talawar MB, Kiran BP, Rao BS, Sugunan S (2000) J Mol Catal A Chem 152:225
27. Sreekumar K, Mathew T, Mirajkar SP, Sugunan S, Rao BS (2000) Appl Catal A Gen 201:L1
28. Sreekumar K, Sugunan S (2002) Appl Catal A Gen 230:245
29. Nishamol K, Rahna KS, Sugunan S (2004) J Mol Catal A Chem 209:89
30. Vijayaraj M, Murugan B, Umbarkar S, Hegde SG, Gopinath CS (2005) J Mol Catal A Chem 231:169
31. Vijayaraj M, Gopinath CS (2007) Appl Catal A Gen 320:64
32. Toledo JA, Valenzuela MA, Bosch P, Armendariz H, Montoya A, Nava N, Vazquez A (2000) Appl Catal A Gen 198:235
33. Toledo JA, Valenzuela MA, Armendariz H, Aguilar-Rios G, Zapata B, Montoya A, Nava N, Salas P, Schifter I (1995) Catal Lett 30:279
34. Ramankutty CG, Sugunan S (2001) Appl Catal A Gen 218:39
35. Mathew T, Shylesh S, Devassy BM, Vijayaraj M, Satyanarayana CV, Rao BS, Gopinath CS (2004) Appl Catal A Gen 273:35
36. Klimkiewicz R, Przybylski K, Baran J, Miśta W (2009) Ind Eng Chem Res 48:6291
37. Reddy VS, RadheShyam A, Dwivedi R, Rai A, Anilkumar M, Chumbale VR, Aswar AS, Prasad R (2006) Indian J Chem Technol 13:493
38. Inoue M, Otsu H, Kominami H, Inui T (1991) J Chem Soc Jpn 7:1036
39. Walerczyk W, Zawadzki M, Grabowska H (2011) Catal Lett 141:592
40. Martin D, Duprez D (1997) J Mol Catal A Chem 118:113
41. Mathew T, Shiju NR, Sreekumar K, Rao BS, Gopinath CS (2002) J Catal 210:405
42. Sparks AK (1972) US Patent 3,670,030
43. Frabetti AF (1975) US Patent 4,041,085
44. Leach BE (1980) US Patent 4,227,024
45. Shamsudeen RK, Nisha K, Sugunan S (2003) React Kinet Catal Lett 79:19
46. Bandyopadhyay R, Singh PS, Rao BS (1997) Appl Catal A Gen 155:27
47. Jacobs JP, Maltha A, Reintjes JGH, Drimal J, Ponrec V, Brongersma HH (1994) J Catal 147:294
48. Sreekumar K, Jyothi TM, Mathew T, Talawar MB, Sugunan S, Rao BS (2000) J Mol Catal A Chem 159:327